

Synthesis and Characterization of Aluminium-Doped Zinc Oxide Nanoparticles via Sol-Gel Method

Rahul S. Nikam¹, Gunwant H. Kurhade², Pooja S. Rindhe³

^{1,2} Department of Physics, Vidnyan Mahavidyalaya, Malkapur, Maharashtra, India

³ Department of Pharmaceutics, Dr. Rajendra Gode College of Pharmacy, Malkapur, Maharashtra, India

DOI: 10.5281/zenodo.15740843

ABSTRACT

The present study focuses on the synthesis and characterization of aluminum-doped zinc oxide (Al:ZnO) nanoparticles using the sol-gel method. The synthesized nanoparticles were systematically characterized using X-ray diffraction (XRD), ultraviolet-visible (UV-Vis) spectroscopy, scanning electron microscopy (SEM), and energy-dispersive X-ray analysis (EDAX). XRD analysis confirmed the formation of nanostructured Al:ZnO with varying crystallite sizes depending on the aluminum doping concentration. UV-Vis spectroscopy revealed a decrease in the optical band gap with increasing aluminum content, indicating successful doping. SEM micrographs demonstrated the morphological features of the nanoparticles, while EDAX confirmed the elemental composition and purity of the synthesized samples. These results collectively validate the successful synthesis and doping of Al into the ZnO lattice and its influence on structural, optical, and morphological properties.

Keyword: - Sol-gel method, Al:ZnO, Nanoparticles.

1. INTRODUCTION:

In the recent era, zinc oxide (ZnO) has attracted significant research interest due to its broad direct band gap (3.37 eV), high exciton binding energy (~60 meV), natural abundance, excellent thermal and mechanical stability, and non-toxicity, making it highly suitable for a wide range of advanced applications.[1, 2]. Zinc oxide (ZnO) is a II–VI group semiconductor that typically crystallizes in a hexagonal wurtzite structure.[3] Zinc oxide possesses key advantages over other semiconductors, including low cost, high chemical durability, environmental friendliness, and strong optical transparency across the visible and near-infrared regions.[4-6]. The physical properties of ZnO, including magnetic, electrical, and optical characteristics, can be modified or tuned by doping and by altering its morphology through appropriate synthesis methods[7, 8]. The electrical and physical properties of ZnO-based materials strongly depend on their synthesis method and composition, particularly the dopant concentration[9]. Aluminum-doped ZnO (AZO) powders were synthesized using the sol-gel process, which is favored for its simplicity, cost-effectiveness, and ability to produce homogeneous, high-purity materials at relatively low temperatures[10, 11].

In this work, AZO powders were prepared by controlling the aluminum doping concentration in the precursor solution. The powders obtained after the sol-gel synthesis were subjected to characterization techniques to analyze their structural, optical, and morphological properties.

2 EXPERIMENTAL PROCEDURE:

2.1 Preparation of Undoped ZnO Nanoparticles (0% AZO):

Zinc oxide nanoparticles were synthesized via the sol-gel method. Glassware was cleaned with aqua regia (HNO₃:HCl = 1:3) and rinsed with distilled water. 10.975 g of zinc acetate was dissolved in 40 mL of distilled water and stirred at 80 °C for 30 min. Then, 5 mL of 0.1 M citric acid was added dropwise, followed by 5 mL of ammonia to initiate gel formation. The resulting gel was aged for 24 h at room temperature, dried at 100 °C for 24 h, ground, and calcined at 600 °C for 4 h to obtain ZnO nano powder.

2.2 Preparation of doped AZO Nanoparticles:

AZO nanoparticles with varying Al doping concentrations (1% and 2%, by weight) were synthesized via the sol-gel method. The required amount of aluminum nitrate was dissolved in 10 mL of distilled water and added to the zinc acetate solution. The mixture was stirred at 80 °C for 30 min, followed by the addition of 5 mL of 0.1 M citric acid and 5 mL of ammonia to form a transparent gel. The gel was aged for 24 h at room temperature, dried at 100 °C for 24 h, ground, and calcined at 600 °C for 4 h to obtain AZO nano powders.

3 RESULTS AND DISCUSSION:

3.1 XRD

3.1.1 XRD of 0 % AZO (undoped ZnO) Nanoparticles:

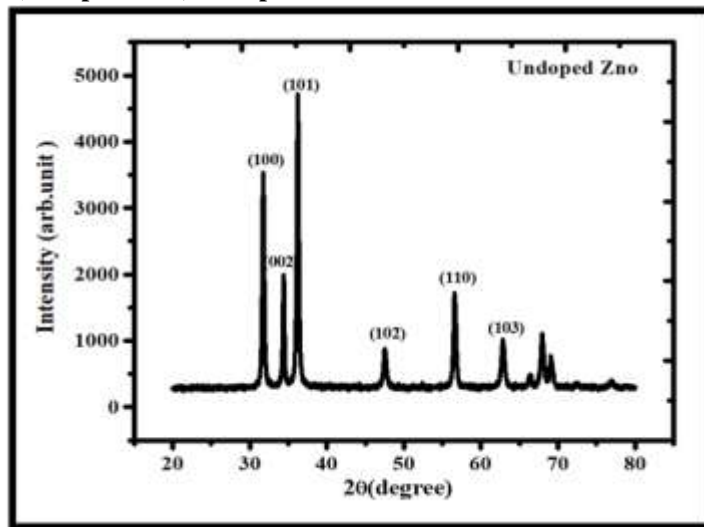


Fig. 1: XRD spectrum of undoped ZnO (0%AZO) nanoparticles.

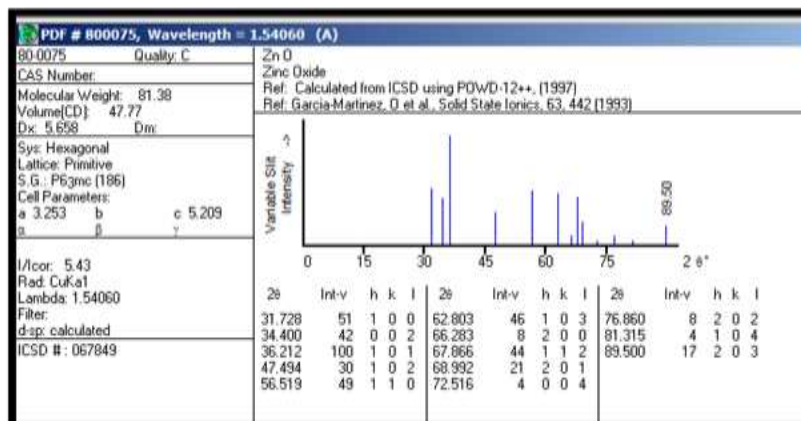


Fig.2: JCPDS data of undoped ZnO (0%AZO) nanoparticles

Determination of ‘d-spacing’: The values of ‘d-spacing’ are calculated by using Bragg’s relation, $n\lambda = 2d \sin\theta$ n = order of diffraction, λ = wavelength of X-rays used d = Interplaner distance, θ = Angle of diffraction

Table 1: Values of d-spacing for undoped ZnO nanoparticles (Both experimental and JCPDS data)

Peak no.	Experimental Data		JCPDS #80-0075 Data	
	2θ (deg.)	d-spacing (nm)	d-spacing (nm)	(hkl)
1	31.78114	0.2816	0.2816	(100)
2	34.45168	0.2604	0.2603	(002)
3	36.27474	0.2477	0.2477	(101)
4	47.58537	0.1911	0.1972	(102)
5	56.635	0.1625	0.1628	(103)

As observed from Table 1, the experimentally obtained d-spacing values closely match the standard JCPDS data up to two decimal places, confirming the formation of the wurtzite phase of ZnO. Furthermore, the absence of any extraneous peaks in the XRD spectrum indicates that the samples are phase-pure and free from detectable impurities.

Determination of Size of the Nanoparticles:

Size of nanoparticles from XRD is determined by using Scherrer formula, which is given as,

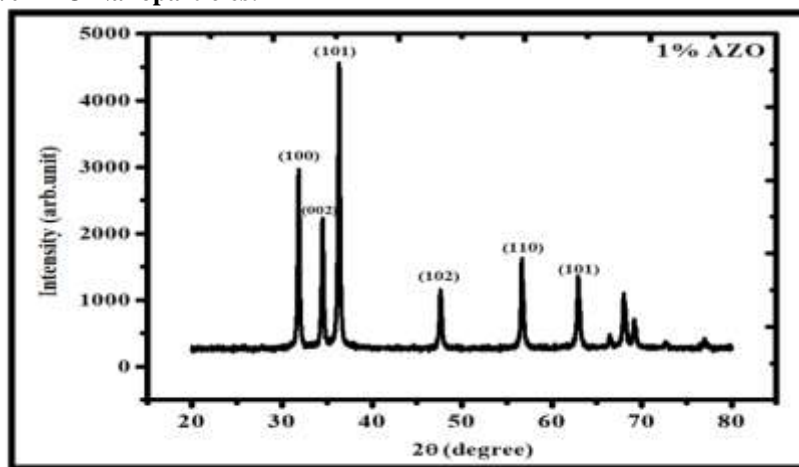
$$d = \frac{0.91\lambda}{\beta \cos \theta}$$

where, d = Size of the nanoparticles, λ = Wavelength of X- rays = 1.54178 Å, β = Full Width at Half Maximum (FWHM) (in radian), θ = Angle of diffraction.

Table 6.2: Determination of size of nanoparticles of undoped ZnO

Peak	θ (deg.)	β (rad.)	Cos θ	Size (nm)
1	15.89057	0.00266	0.961825	54.844
2	17.22584	0.002701	0.95519	54.382
3	18.13737	0.002864	0.950363	51.550
4	23.79269	0.00292	0.915096	52.514
5	28.3175	0.003005	0.880451	53.020
6	31.46593	0.003385	0.853096	48.589
Average size of nanoparticles = 52.48 nm				

The broadening of diffraction peaks in the XRD spectrum indicates the formation of nanoparticles. The average crystallite size of undoped ZnO (0% AZO), calculated using the Scherrer formula, was found to be approximately 52.48 nm[12].

3.1.2 XRD of 1% AZO Nanoparticles:**Fig. 3** XRD spectrum of 1.0% AZO nanoparticles**Table 2:** Determination of size of 1.0% AZO nanoparticles

Peak	θ (deg.)	β (rad.)	Cos θ	Size (nm)
1	15.92715	0.0022719	0.96165007	64.218
2	17.25517	0.0023067	0.95503848	63.687
3	18.17186	0.0024356	0.95017549	60.625
4	23.82002	0.0028205	0.91490371	54.370
5	28.34999	0.0030864	0.88018251	51.646
6	31.48301	0.0033801	0.85294051	48.664
Average size of nanoparticles = 57.20 nm				

For 1.0% Al-doped ZnO (AZO) nanoparticles, the average crystallite size was found to be 57.20 nm. A decreasing trend in particle size was observed with increasing doping concentration. Additionally, the absence of any secondary or extraneous peaks in the XRD spectra confirms the successful formation of phase-pure wurtzite structured ZnO.

3.1.3 XRD of 2% AZO Nanoparticles:

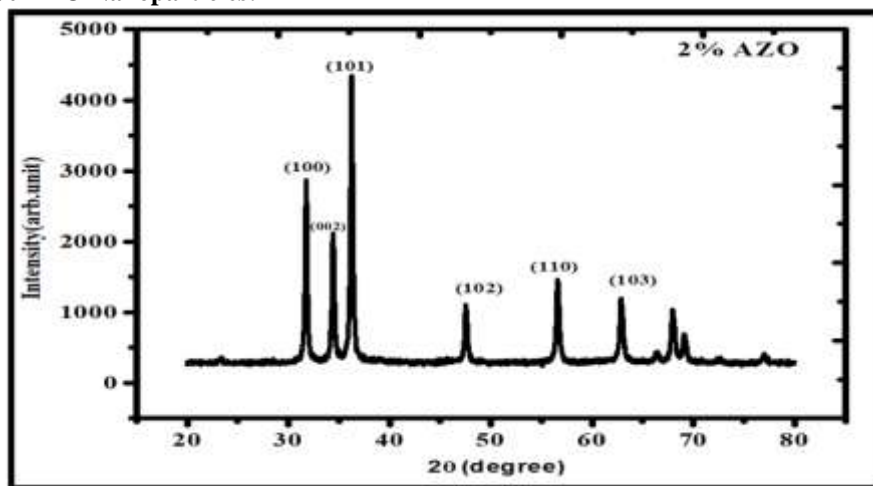


Fig. 4: XRD spectrum of 2.0% AZO nanoparticles

Table 3: Determination of size of 2.0% AZO nanoparticles

Peak	θ (deg.)	β (rad.)	$\cos \theta$	Size (nm)
1	15.88498	0.0023952	0.96185158	60.899
2	17.21403	0.0025445	0.95525099	57.721
3	18.12986	0.0025566	0.95040362	57.742
4	23.7799	0.0030201	0.91518604	50.761
5	28.31168	0.0031999	0.88049947	49.7960
6	31.44934	0.0036633	0.85324701	44.886
Average size of nanoparticles = 53.63 nm				

For 2.0% Al-doped ZnO (AZO) nanoparticles, the average crystallite size was found to be 53.63 nm, indicating a further reduction in size with increased doping concentration. As with the previous samples, no extraneous peaks were observed in the XRD spectra, confirming the formation of a phase-pure wurtzite structure of ZnO[13].

3.1.4 Comparison of XRD Spectra of all the Samples:

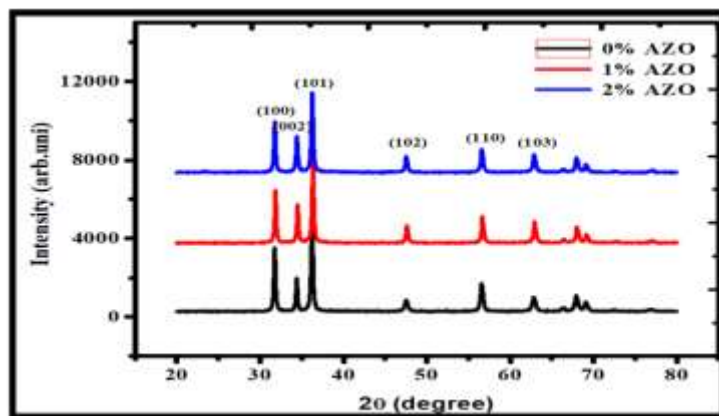


Fig. 5: Comparison of the XRD spectra of 0%, 1% and 2% AZO nanoparticles.

A comparative analysis of the XRD spectra for 0%, 1%, and 2% AZO samples reveals no extraneous peaks corresponding to aluminum oxide, confirming the formation of phase-pure wurtzite ZnO in each case and indicating high sample purity. Notably, with increasing Al doping, a slight shift in the diffraction angle and broadening of the peaks is observed. To further investigate this behavior, the most intense diffraction peak, namely the (101) plane, was examined for all samples, as shown in Figure 5. This shift and broadening can be attributed to lattice distortion and the incorporation of Al ions into the ZnO crystal lattice.

Table 4: Comparison of the size of all samples

Sample	Size(nm)
0% AZO	52.48
1% AZO	57.20
2% AZO	53.63

The X-ray diffraction (XRD) analysis confirms that all observed diffraction peaks match well with the JCPDS card no. #80-0075, indicating the formation of the body-centered hexagonal wurtzite phase of ZnO. The broadening of diffraction peaks clearly suggests the formation of nanoparticles. A comparative study of the most intense diffraction peak, (101), across all samples reveals a systematic increase in the peak width (β , FWHM) with increasing doping concentration, which correlates with a decrease in average crystallite size. The average particle sizes calculated using the Debye-Scherrer formula are 52.48 nm for 0% AZO, 57.20 nm for 1% AZO, and 53.63 nm for 2% AZO, as shown in Table 4. Interestingly, an initial increase in size is observed at 0.5% doping, which may be attributed to the interstitial incorporation of Al^{3+} ions (ionic radius = 0.53 Å) into the ZnO lattice (Zn^{2+} ionic radius = 0.74 Å). This results in lattice expansion due to the added strain. However, at higher concentrations (1% to 2%), the substitutional incorporation of smaller Al^{3+} ions in place of Zn^{2+} ions likely leads to lattice contraction and a systematic reduction in particle size. Correspondingly, a decrease in lattice parameters is observed, further supporting the substitutional doping mechanism at higher Al content[12].

3.2 UV-vis Reflectance Spectra:

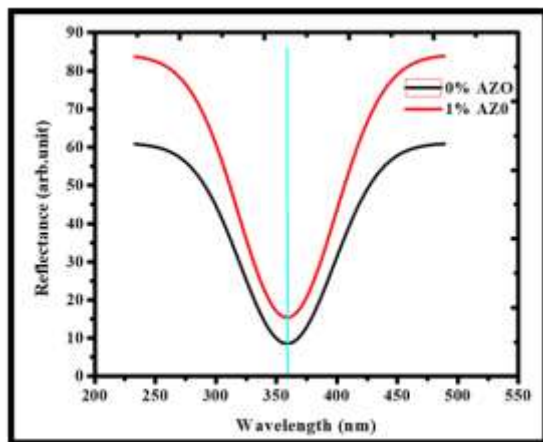
**Fig. 6 : UV-Vis Reflectance Spectra**

Figure 6 presents the reflectance spectra of undoped and aluminum-doped ZnO (AZO) nanoparticles. A noticeable redshift in the reflection wavelength is observed with increasing Al doping concentration, indicating a shift towards longer wavelengths. This shift suggests a reduction in the optical band gap energy with doping. Specifically, the band gap decreases from 3.256 eV for undoped ZnO to 3.164 eV for 1% AZO, which is attributed to the incorporation of Al^{3+} ions into the ZnO lattice, modifying its electronic structure and optical absorption behavior[14].

Tauc Method to determine Band-gap Energy from UV-vis Reflectance Spectra:

The reflectance spectra of all the samples are shown in Fig. 6.13. The corresponding band-gap energies E_g were determined using the Tauc equation. We have taken the values of $\left\{ hv \left[\ln \left(\frac{R_{\max} - R_{\min}}{R - R_{\min}} \right) \right]^2 \right\}$ on y axis and hv (eV) on the x-axis. Extrapolating the linear region of the $\left\{ hv \left[\ln \left(\frac{R_{\max} - R_{\min}}{R - R_{\min}} \right) \right]^2 \right\}$ Vs hv (eV) curve to the energy axis, the optical band-gap energy of the sample was obtained. A Tauc plot for ZnO sample is shown in the following Fig. 7 (a,b), along with the corresponding band-gap energy. The band-gap energy of ZnO is about 3.256eV and that of 1% AZO is about 3.164 eV.

For undoped ZnO:

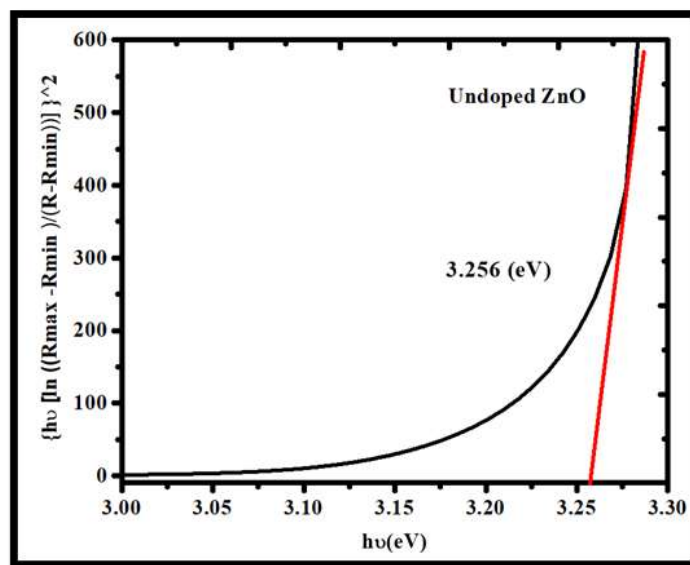


Fig. 7 (a): Tauc Plot of Undoped ZnO Nanoparticle

For 1% AZO:

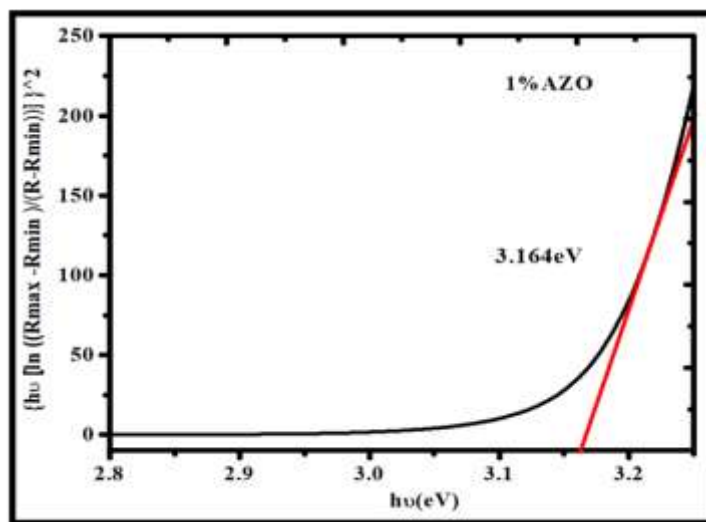


Fig. 7 (b): Tauc Plot of 1% AZO Nanoparticles

Result of UV-Vis Reflectance Spectra:

Then we plot the graph of $\left\{ hv \left[\ln \left(\frac{R_{\max} - R_{\min}}{R - R_{\min}} \right) \right] \right\}^2$ Vs hv (eV) and extrapolate the curve to the energy axis, the optical band-gap of the sample is obtained. The band-gap energy of ZnO is 3.25 eV and that of 1% AZO is 3.16 eV. This is because Al is a conductive material and it contains free electrons. Thus, as Al doping increases the band-gap energy decreases making the particles more conducting[14].

3.3 Scanning Electron Microscopy (SEM):

SEM is used to determine the morphology (texture), average size and chemical composition of the samples. The morphology and average size of synthesized undoped AZO nanoparticles and 1% AZO nanoparticles is determined by SEM.

1) SEM image of undoped ZnO (0% AZO):

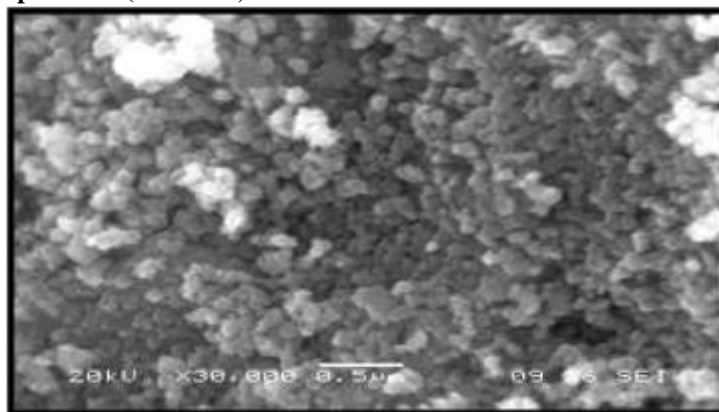


Fig. 8(a): SEM of 0% AZO

2) SEM image of 1% AZO:

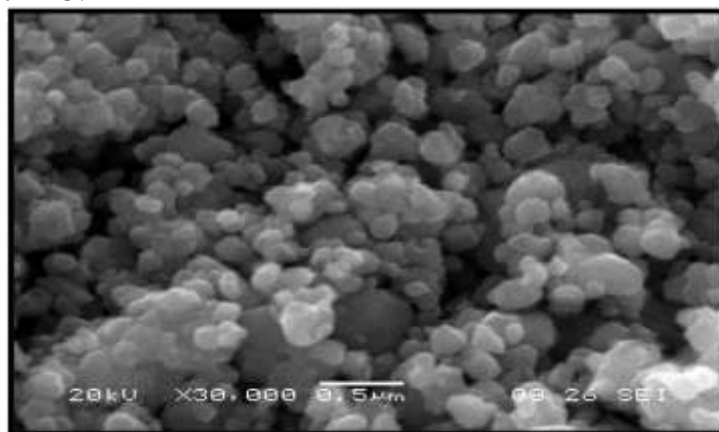


Fig. 8 (b): SEM of 1% AZO

From the SEM images, it can be concluded that both undoped and aluminum-doped ZnO (AZO) nanoparticles exhibit a hexagonal morphology with a uniform distribution. This consistent shape and homogeneous dispersion of nanoparticles indicate successful synthesis and doping without significant agglomeration or morphological changes[15].

3.4 Energy Dispersive X-ray analysis (EDAX):

Energy Dispersive X-Ray Analysis (EDAX) is an x-ray technique used to identify the elemental composition of materials.

1) EDAX of undoped AZO nanoparticles:

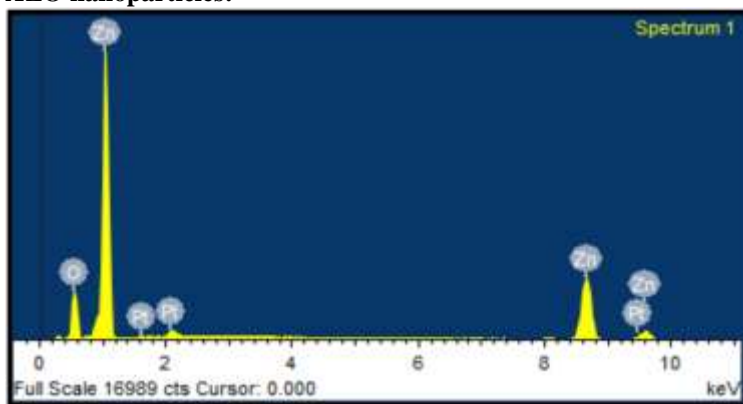


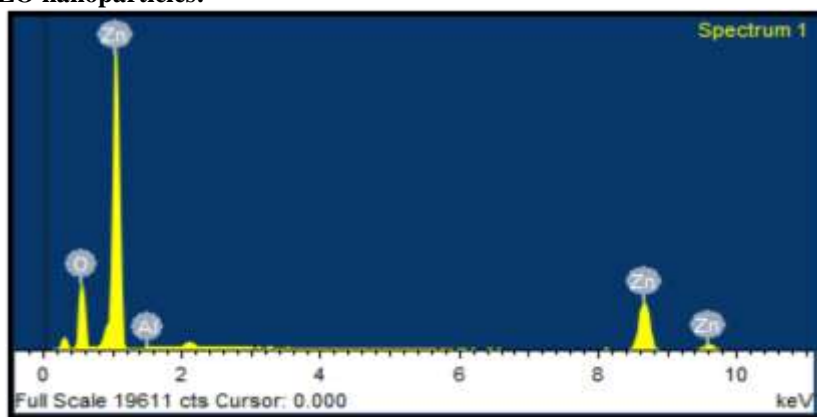
Fig. 9(a) EDAX of undoped ZnO

Table 5: EDAX result of undoped ZnO nanoparticles

Element	Weight%	Atomic%
O K	31.64	65.42
Zn	68.36	34.58

The EDAX analysis of the sample reveals the presence of only zinc and oxygen elements, confirming the absence of any impurities. However, the atomic percentage ratio of zinc to oxygen is found to be 0.53:1, deviating from the ideal 1:1 stoichiometric ratio of ZnO. This discrepancy arises due to the formation of zinc vacancies at the nanoscale, which disrupt the stoichiometry of the material. In contrast, bulk ZnO maintains the ideal 1:1 ratio because of its stable crystal lattice structure[16].

2) EDAX of 1%AZO nanoparticles:

**Fig.9 (b)** EDAX of 1% AZO**Table 6:** EDAX result of 1% AZO nanoparticles

Element	Weight%	Atomic%
O K	41.47	74.14
Al K	0.37	0.39
Zn	58.15	25.45

The EDAX results confirm that the samples contain only oxygen, zinc, and aluminum, with no other impurities detected. From the SEM analysis, it can be concluded that both undoped and aluminum-doped zinc oxide nanoparticles exhibit a hexagonal shape with uniform distribution. The EDAX findings further support the purity of the synthesized nanoparticles, indicating the absence of any extraneous elements in both undoped and aluminum-doped ZnO samples[17].

4. CONCLUSION

In this study, undoped and aluminium-doped zinc oxide (AZO) nanoparticles were successfully synthesized using the sol-gel method, which offers simplicity, low cost, and the ability to produce mono-sized particles. XRD analysis confirmed the formation of a pure wurtzite phase for all samples. The particle size initially increased at 0.5% Al doping due to interstitial incorporation of Al ions but decreased with further doping (1–3%) as Al^{3+} substituted Zn^{2+} in the lattice. SEM revealed uniform hexagonal morphology, and EDAX confirmed high purity of the samples. UV-Vis measurements showed a decrease in optical band-gap energy with increasing Al content from 3.25 eV for pure ZnO to 3.16 eV for 1% AZO indicating improved conductivity due to the presence of free electrons from conductive Al. The Tauc plot precise determination of the optical band-gap. These findings confirm that Al doping effectively tailors the structural and optical properties of ZnO, making AZO nanoparticles suitable for optoelectronic and sensor applications.

ACKNOWLEDGMENT

I sincerely thank the Principal of Vidnyan Mahavidyalaya, Malkapur, for providing the necessary research facilities. I am also grateful to Dr. Rajendra Gode, Principal of the College of Pharmacy, for his valuable guidance and support. Additionally, I express my heartfelt thanks to Savitribai Phule Pune University for granting access to advanced characterization facilities, including XRD, SEM, UV-Visible spectroscopy, and EDAX.

REFERENCES:

- [1] S. Raha and M. Ahmaruzzaman, "ZnO nanostructured materials and their potential applications: progress, challenges and perspectives," *Nanoscale Advances*, vol. 4, no. 8, pp. 1868-1925, 2022.
- [2] P. Kumari, A. Srivastava, R. K. Sharma, D. Sharma, and S. K. Srivastava, "Zinc oxide: a fascinating material for photovoltaic applications," in *Nanomaterials for innovative energy systems and devices*: Springer, 2022, pp. 173-241.
- [3] A. Srivastava and A. Katiyar, "Zinc oxide nanostructures," in *Ceramic Science and Engineering*: Elsevier, 2022, pp. 235-262.
- [4] V. Kumar, O. Ntwaeaborwa, T. Soga, V. Dutta, and H. Swart, "Rare earth doped zinc oxide nanophosphor powder: a future material for solid state lighting and solar cells," *Acs Photonics*, vol. 4, no. 11, pp. 2613-2637, 2017.
- [5] H. Wen *et al.*, "Advancements in transparent conductive oxides for photoelectrochemical applications," *Nanomaterials*, vol. 14, no. 7, p. 591, 2024.
- [6] W. S. Shen, Y. K. Wang, and L. S. Liao, "Near-Infrared Quantum Dots for Electroluminescence: Balancing Performance and Sustainability," *Laser & Photonics Reviews*, p. 2401947, 2025.
- [7] D. K. Sharma, S. Shukla, K. K. Sharma, and V. Kumar, "A review on ZnO: Fundamental properties and applications," *Materials Today: Proceedings*, vol. 49, pp. 3028-3035, 2022.
- [8] B. G. Shohany and A. K. Zak, "Doped ZnO nanostructures with selected elements-Structural, morphology and optical properties: A review," *Ceramics International*, vol. 46, no. 5, pp. 5507-5520, 2020.
- [9] M. Ahmad and J. Zhu, "ZnO based advanced functional nanostructures: synthesis, properties and applications," *Journal of Materials chemistry*, vol. 21, no. 3, pp. 599-614, 2011.
- [10] S. HUSSAIN, F. WAHAB, M. USAMA, A. ARSHAD, H. KHAN, and S. GUL, "Materials Chemistry: Properties And Applications," *Chemistry: The Modern Approach*, p. 29, 2024.
- [11] P. Zhang, R. Hong, Q. Chen, W. Feng, and D. Badami, "Aluminum-doped zinc oxide powders: synthesis, properties and application," *Journal of Materials Science: Materials in Electronics*, vol. 25, pp. 678-692, 2014.
- [12] H. Q. AL-Arique, S. S. AL-Qadasy, N. M. Kaawash, S. Chishty, and K. A. Bogle, "Study the characterization of ZnO and AZO films prepared by spray pyrolysis and the effect of annealing temperature," *Optical Materials*, vol. 150, p. 115261, 2024.
- [13] N. Srinatha, K. R. Kumar, M. S. Kumar, K. V. Pattar, A. Madhu, and B. Angadi, "Combustion synthesis of Al-doped ZnO nanoparticles using a new fuel and the study of its structural, micro-structural and optical properties," *Applied Nanoscience*, vol. 11, pp. 1197-1209, 2021.
- [14] J. Ungula, "Formation and characterization of novel nanostructured un-doped and Ga-doped ZnO transparent conducting thin films for photoelectrode," University of the Free State (Qwaqwa Campus), 2018.
- [15] M. Asif *et al.*, "Synthesis, Characterization, and Evaluation of the Antimicrobial and Anticancer Activities of Zinc Oxide and Aluminum-Doped Zinc Oxide Nanocomposites," *Pharmaceuticals*, vol. 17, no. 9, p. 1216, 2024.
- [16] S. S. Gaikwad *et al.*, "Oxygen induced strained ZnO nanoparticles: an investigation of Raman scattering and visible photoluminescence," *Journal of Materials Chemistry C*, vol. 2, no. 35, pp. 7264-7274, 2014.
- [17] C. P. Liu and G. R. Jeng, "Properties of aluminum doped zinc oxide materials and sputtering thin films," *Journal of Alloys and Compounds*, vol. 468, no. 1-2, pp. 343-349, 2009.